D D

RESEARCH INSTITUTE FOR HIGH ENERGY PHYSICS

REPORT SERIES

HU - SEFT R 1994 - 13

The Effect of the L3 Tracking Upgrade on the W Mass and Triple Boson Coupling Measurements

P. Laurikainen, A. Lilja, R. Ostonen, C. Spartiotis

Research Institute for High Energy Physics
University of Helsinki, Finland

SEFT

ISSN 0788-3587

UNIVERSITY OF HELSINKI
RESEARCH INSTITUTE FOR HIGH ENERGY PHYSICS
P.O.Box 9 • FIN-00014 UNIVERSITY OF HELSINKI • FINLAND

The Effect of the L3 Tracking Upgrade on the W Mass and Triple Boson Coupling Measurements

P. LAURIKAINEN, A. LILJA, R. OSTONEN, C. SPARTIOTIS

Abstract

We present a study of determining the influence of the L3 tracking system performance on the precision of W mass and γWW, ZWW coupling measurements. For the W mass resolution we set an upper limit on the expected improvement. The increase in precision of the triple boson coupling measurements is estimated for different theoretical assumptions, which lead to non-standard couplings.

1 Introduction

The precise determination of the W boson mass and the γWW, ZWW couplings are among the main objectives of the LEP200 project. If the mass of the top quark is known, the W mass measurement will constrain the Standard Model Higgs boson mass. On the other hand, the determination of triple boson couplings will provide a test of the non-Abelian nature of the Standard Model. The precision of these measurements depends on the quality of the detector systems, therefore studies are necessary to estimate the errors caused by the detector performance.

In this paper we study the effect of the performance of the tracking system on the precision of the W mass and triple boson coupling measurements. We compare the existing tracking system of L3 with one of the tracking systems, planned for LEP200 upgrade.

In the first part of the paper the determination of W mass is studied, we describe a method based only on the tracking system. The described method, however, is not competitive with the methods that use also the information from the calorimeters, but it will give an upper limit for the improvement in W mass resolution that one expects from replacing the existing tracker with the upgraded one.

The second part of the work is devoted to the triple boson coupling measurements, based on fitting the experimentally obtained angular differential cross section for W pair production with a theoretical distribution. We study four different models and compare the results obtained for the existing L3 tracker and for the tracker upgrade planned for LEP200. We obtain an estimate for the improvement in determining the triple boson couplings.

2 Event Generation and Simulation of the Trackers

For the present study we used the L3 EGWW V2.07 generator to simulate the process $e^+e^- \longrightarrow$ W^+W^-. This is a modified version of the LEPWW generator, based on the formulae of K. Hagiwara *et al.* [1]. The generator values for the mass and width of W were $M_W = 80.44$ GeV and $\Gamma_W = 2.20$ GeV. The generation included also initial state radiation.

The total cross-section for the process $e^+e^- \longrightarrow W^+W^-$ was taken to be 18 pb [2]. For LEP200 the integrated luminosity of 500 pb^{-1} was assumed, thus the expected number of W^+W^- events at LEP200 will be $\sim$ 9000. Table 1 gives the number of different final states for the W^+W^- events at LEP200.

Process	No. of events.
$W^+W^- \longrightarrow q\bar{q}q\bar{q}$	4410 (49%)
$W^+W^- \longrightarrow \tau\nu q\bar{q}$	1260 (14%)
$W^+W^- \longrightarrow e(\mu)\nu q\bar{q}$	2520 (28%)
$W^+W^- \longrightarrow l\nu l\nu$	810 (9%)

Table 1: W^+W^- events at LEP200.

In this work we compare the existing tracking system of L3 (the SMD and TEC) with one of those proposed for Stage II at LEP200. Tables 2 and 3 provide the specifications of the existing tracking system and the design values for the Phase II tracker (SIO: Silicon Outer layer, SIFT: Silicon Forward Tracker).

The more precise description of the upgrade can be found in [3].

The performance of the trackers was simulated according to the resolutions given in [3].

	Phase I	Phase II
Barrel Region		
$r_{\text{beam tube}}$(cm)	5.30	5.30
X_0 of beam tube(%)	0.6	0.6
r_1 SMD(cm)	6.10	6.10
r_2 SMD(cm)	7.80	7.80
z SMD(sensitive)(cm)	$\pm$14.00	$\pm$ 28.00
$\sigma_{R\phi}$ SMD(μm)	10	10
σ_z SMD(μm)	15	15
X_0 of SMD(total)(%)	1.0	1.0
r_{inner} TEC(cm)	9.00	9.00
r_{outer} TEC(cm)	45.25	48.00
z TEC(sensitive)(cm)	$\pm$49.10	$\pm$68.00
$r_{\text{first wire}}$ inner TEC(cm)	10.98	10.05
$r_{\text{last wire}}$ inner TEC(cm)	14.34	16.75
Number of inner wires	8	8
$r_{\text{first wire}}$ outer TEC(cm)	17.28	18.80
$r_{\text{last wire}}$ outer TEC(cm)	42.72	46.7
Number of outer wires	54	32
$\sigma_{R\phi}$ TEC(μm)	70	55
X_0 of inner TEC wall(%)	1.0	1.0
X_0 of outer TEC wall(%)	10.0	3.0
X_0 of TEC endflange(%)	140.0	$<$30.0
r SIO(cm)	–	50.50
z SIO(sensitive)(cm)	–	$\pm$60.0
$\sigma_{R\phi}$ SIO(μm)	–	15
σ_z SIO(μm)	–	50
X_0 of SIO(total)(%)	–	1.0

Table 2: Specifications of the existing Phase I (TEC+SMD) tracking system and the design values of the Phase II (New-TEC+Ext.-SMD+SIO+SIFT) tracking system.

	Phase I	Phase II
F/B Region		
r_{outer} SIFT(cm)	–	48.2
r_{inner} SIFT(cm)	–	14.50
z SIFT(cm)	–	at $\pm$ 70.00
σ_ϕ SIFT(μm)	–	15
σ_R SIFT(μm)	–	50
X_0 of SIFT(total) (%)	–	1.0

Table 3: The design values of SIFT to be installed during the Phase II upgrade. (See the previous Table for the explanation of Phase I and Phase II).

3 W Mass Reconstruction

3.1 Methods for W Mass Measurement

There exist several methods to measure W mass at LEP200 in the process $e^+e^- \longrightarrow W^+W^-$:

- W mass measurement from the threshold behaviour of the total cross-section $\sigma(e^+e^- \longrightarrow W^+W^-)$, (the estimated error $\delta M_W = 100 - 130$ MeV [4]);
- W mass measurement from the end point of the lepton energy spectrum, ($\delta M_W = 300 - 500$ MeV [4]);
- W mass measurement by reconstructing the W hadronic decay products.

In this work we concentrate on the third method, which is based on the reconstruction of energy and momentum of the W hadronic decay products and thereafter estimating the energy and momentum of the W, which are then used to calculate W mass.

Calorimetric Approach

In the calorimetric approach, after one has assigned some two jets to originate from the same W, the energy of these jets can be measured in the calorimeter and assuming the momentum and energy of the jets to be equal, the W mass can be estimated from

$$M^2_{W,rec} = 2E_1E_2(1 - \cos\theta_{12}), \tag{1}$$

where E_1 and E_2 are the energies of the jets and θ_{12} is the angle between the jet axis. The obtained value $M_{W,rec}$ can then be rescaled using the "mass rescaling" method [4], correcting for the energy losses in the detector:

$$M_W = M_{W,rec}\frac{E_{beam}}{E_1 + E_2}. \tag{2}$$

The described process is repeated for each event. The obtained invariant mass plot can then be fitted with a Breit–Wigner for the peak and a polynomial for the background, thus obtaining the W mass.

It is possible to apply energy and momentum conservation together with the assumption of equality of the two W masses to obtain improved estimates for the jet energies E_1 and E_2 and for the angle θ_{12}. This method is investigated thoroughly in [5], where the precision of W mass measurement is also studied as a function of the tracker resolution. In this paper we focus on the tracker approach described below.

Tracker Approach

One can measure the energy of the charged decay products more precisely using the tracking system (the tracker approach). In the following description we assume that all the decay products originate from the same W, we discuss the problem of assigning jets to one particular W later.

In the process $e^+e^- \longrightarrow W^+W^-$, each W gains a total energy, approximately equal to the beam energy E_{beam} (see Figure 1):

$$E_{cms} = 2E_{beam} \approx 2E_W. \tag{3}$$

The small deviations from this value are caused by radiative corrections and the unequality of the two W masses. Assuming all charged particles to have pion mass and measuring their

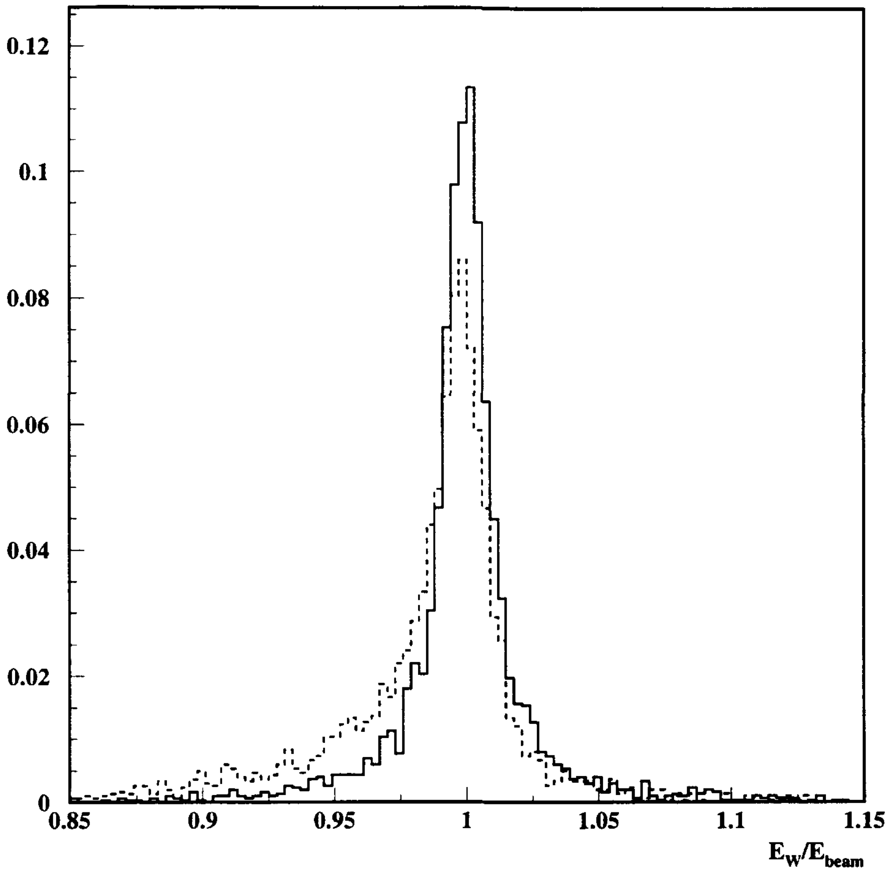

Figure 1: The energy of a W in the process $e^+e^- \longrightarrow \mathrm{W^+W^-}$. The solid line denotes the distribution without initial state radiation, the dashed line includes initial state radiation. The distribution is normalized to the number of events.

three-momenta, using only the tracking system, one can find the energy (E_{ch}) of all charged particles.

A correction factor α is introduced to correct for the neutral particles and particles that were not detected:

$$E_{\mathrm{W}} = \alpha E_{ch}, \tag{4}$$

$$p_{\mathrm{W}} = \alpha p_{ch}. \tag{5}$$

One can determine α from (3) and (4), since E_{beam} is known. Thereafter, using (5), the W mass can be calculated from:

$$M_{\mathrm{W}}^2 = E_{\mathrm{W}}^2 - p_{\mathrm{W}}^2. \tag{6}$$

The obtained invariant mass plot is then fitted with a Breit–Wigner for the peak and a second order polynomial for the background.

The described method can be used for both, the hadronic ($\mathrm{W^+W^-} \longrightarrow \mathrm{q\bar{q}q\bar{q}}$) and semileptonic ($\mathrm{W^+W^-} \longrightarrow e(\mu)\nu\mathrm{q\bar{q}}$) events. The procedure is straightforward in the semileptonic case:

after identifying the lepton, the remaining particles will be assigned to the W, which has decayed hadronically.

In case of pure hadronic mode, one has to assign the resulting jets correctly to the two different W's. For 4-jet events it is possible to select a combination of jet pairs (ij and kl) so, that the energies observed in the calorimeter for the jet pairs (E_{ij}, E_{kl}) are the closest to beam energy:

$$|E_{ij} - E_{beam}| + |E_{kl} - E_{beam}| \rightarrow \text{min.} \tag{7}$$

Alternatively one could choose a combination of jet pairs, which invariant masses are closest to $M_{\mathrm{W}0}$:

$$|M_{\mathrm{W},ij} - M_{\mathrm{W}0}| + |M_{\mathrm{W},kl} - M_{\mathrm{W}0}| \rightarrow \text{min,} \tag{8}$$

where $M_{\mathrm{W}0}$ is a rough estimate of M_{W}.

3.2 Results of Simulations

In our study we used the same number of $\mathrm{W}^+\mathrm{W}^- \longrightarrow e(\mu)\nu\mathrm{q}\bar{\mathrm{q}}$ events that one expects to get from LEP200 (~ 2500). The process $\mathrm{W}^+\mathrm{W}^- \longrightarrow \tau\nu\mathrm{q}\bar{\mathrm{q}}$ can be used effectively only if the τ does not decay hadronically ($\sim 35\%$), giving additional 400 events. Simulations were carried out for two beam energies: 90 GeV and 100 GeV.

For identifying a semileptonic event one needs to detect a high energy lepton ($p > 20$ GeV). This can be done effectively by using the information from the electromagnetic calorimeter and muon chambers, which cover the polar angle between $12^\circ < \theta < 168^\circ$.

Suitable cuts can be introduced to obtain the best mass estimate. The most relevant cut seems to be the minimal number of charged tracks per event ($N_{ch,min}$), below which the event is rejected: for a small $N_{ch,min} < 8$ the W peak will be distorted, since the correction factor α is badly determined (the more charged tracks there are in an event, the better α will be determined); for large $N_{ch,min} > 12$ the losses in statistics will become significant. The distribution of the number of charged tracks per event is presented in Figure 2. According to our simulations, $N_{ch,min} \approx 10$ appears to be good.

To summarize, we list all the cuts used for the semileptonic events:

- Neutral particles and particles with $p < 0.5$ GeV were considered as undetected (see also Figure 3);
- Particles with $\theta < 24^\circ$, or $\theta > 156^\circ$ (the present tracking system) and $\theta < 13^\circ$, or $\theta > 167^\circ$ (the tracking upgrade) were considered as undetected.

The event was accepted in the analysis, if:

- An energetic lepton ($p > 20$ GeV) with $12^\circ < \theta_{lepton} < 168^\circ$ was observed;
- At least 10 charged tracks were observed.

The results of the estimates for the precision of the W mass measurement using the method described above are summarized in Table 4.

In Figures 4 and 5 we present the obtained invariant mass plot for $E_{beam} = 90$ GeV and 100 GeV respectively.

As can be seen, the replacement of the existing tracking system with the upgraded one will provide an increase in the precision of W mass measurement of about 10–12%.

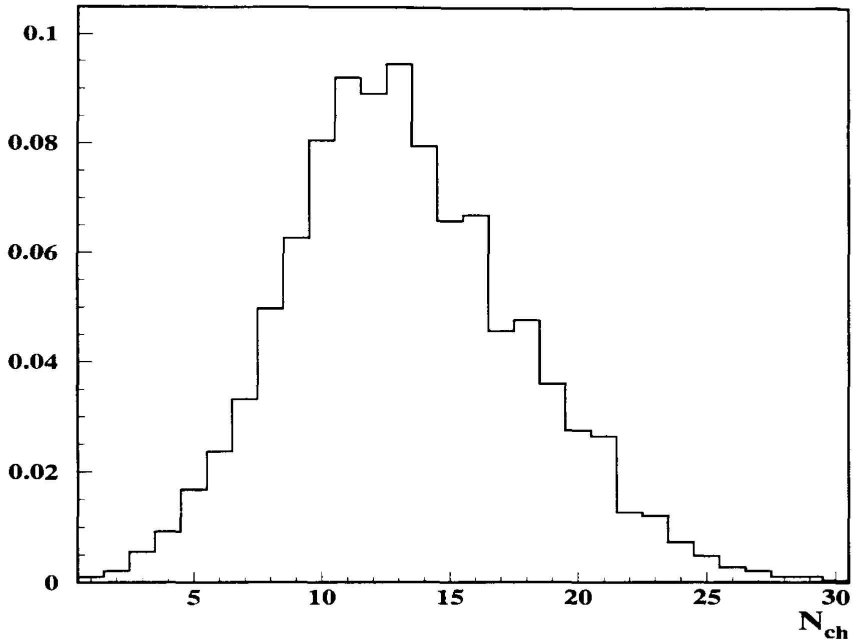

Figure 2: The number of charged tracks ($p > 0.5$ GeV) per event for the process $W^+W^- \longrightarrow e(\mu)\nu q\bar{q}$ for $E_{beam} = 100$ GeV. The lepton track is not included. The distribution is normalized to the number of events.

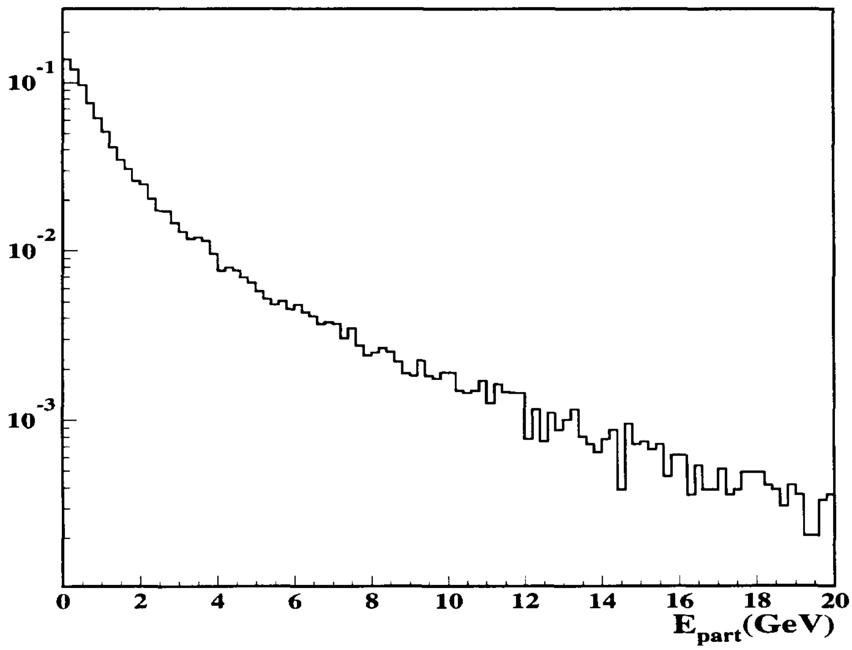

Figure 3: The energy spectrum of hadrons in the process $W^+W^- \longrightarrow e(\mu)\nu q\bar{q}$ for $E_{beam} =$ 100 GeV. The distribution is normalized to the number of particles.

Tracking system	δM_W (E_{beam} = 90 GeV)	δM_W (E_{beam} = 100 GeV)
The existing L3 tracking system	0.136 GeV	0.200 GeV
The L3 tracking upgrade	0.120 GeV	0.181 GeV
Improvement	12%	10%

Table 4: The error of M_{W} measurements in the process $e^+e^- \longrightarrow \mathrm{W}^+\mathrm{W}^- \longrightarrow e(\mu)\nu q\bar{q}$.

The error on the obtained W mass value is also dependent on beam energy. For the 100 GeV case the errors on W mass are about a factor of 1.5 greater. This is due to the fact that in the 100 GeV case the possible values for the reconstructed W mass satisfy $M_{\mathrm{W},rec} < 100$ GeV, whereas in the 90 GeV case $M_{\mathrm{W},rec} < 90$ GeV. The result of this is that with $E_{beam} = 100$ GeV the mass peak is lower and has a tail extending to the values up to 100 GeV, but with $E_{beam} =$ 90 GeV the mass peak is higher and the tail at high reconstructed mass values is missing, see also Figures 4 and 5. Therefore the fitting procedure leads to larger errors for $E_{beam} = 100$ GeV.

The effect of different cuts applied are summarized in Tables 5 and 6.

	Present tracking system	Tracking upgrade
Total number of rejected events	679 (23%)	491 (17%)
Events rejected due to Cut #1	611 (21%)	423 (15%)
Events rejected due to Cut #2	68 (2%)	68 (2%)

Table 5: Number of events rejected according to the different cuts (for 2900 generated events), $E_{beam} = 90$ GeV. Cut #1: less than 10 charged tracks; Cut #2: $\theta_{lepton} < 12°$ ($\theta_{lepton} > 168°$).

	Present tracking system	Tracking upgrade
Total number of rejected events	671 (23%)	460 (16%)
Events rejected due to Cut #1	586 (20%)	384 (13%)
Events rejected due to Cut #2	76 (3%)	76 (3%)

Table 6: Number of events rejected according to the different cuts (for 2900 generated events), $E_{beam} = 100$ GeV. Cut #1: less than 10 charged tracks; Cut #2: $\theta_{lepton} < 12°$ ($\theta_{lepton} > 168°$).

Part of the increase in precision is due to the increase of statistics, since the new setup will cover a larger solid angle, thus making it possible to detect a larger number of charged particles. To study this we used the following procedure. We compared the values of δM_{W} for the present and upgraded tracking systems, requiring the number of events to be the same after all the cuts had been applied. Taking $E_{beam} = 90$ GeV and requiring approximately 2200 events in both

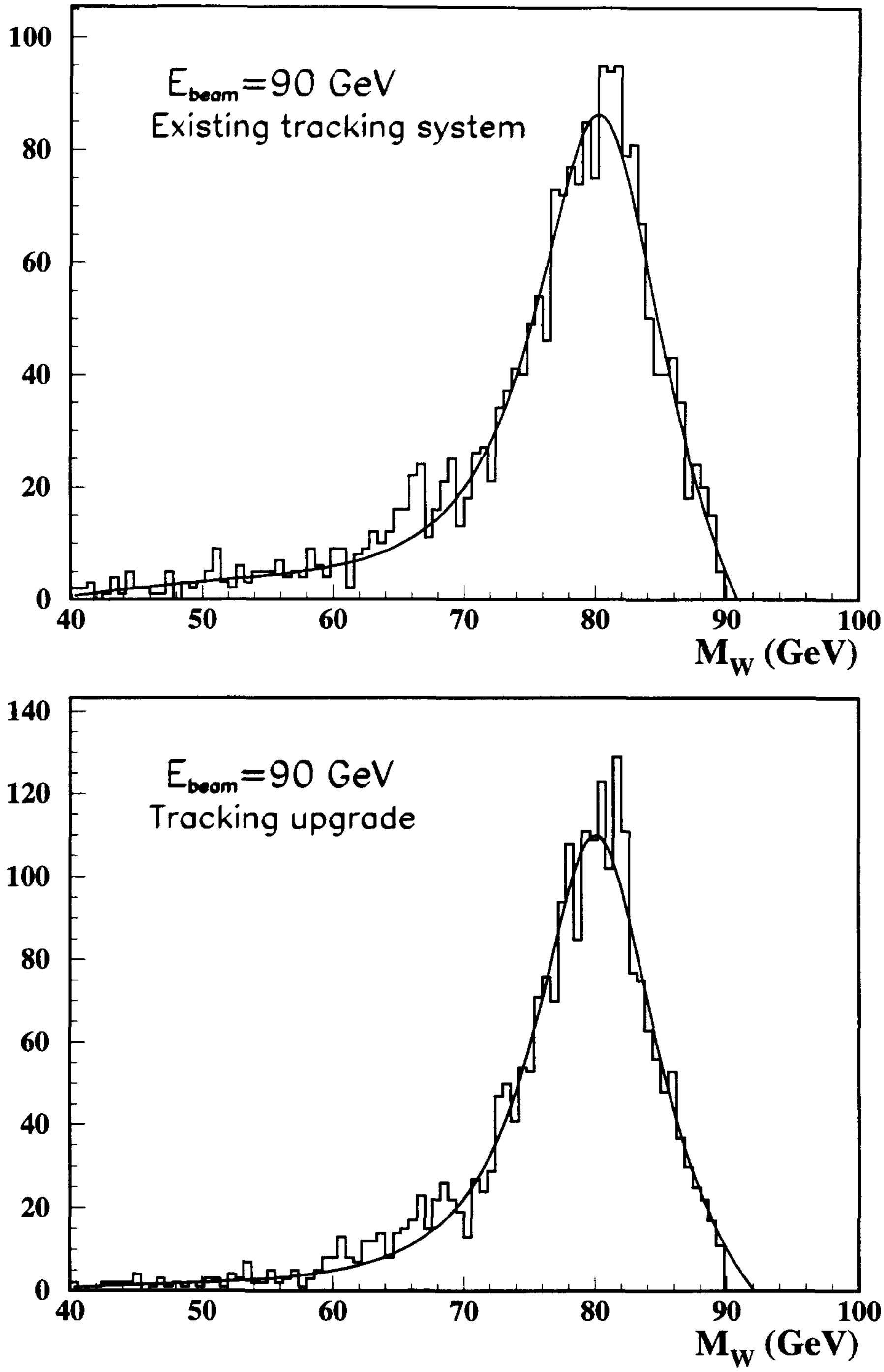

Figure 4: The reconstructed W mass in the process $e^+e^- \longrightarrow W^+W^- \longrightarrow e(\mu)\nu q\bar{q}$ (E_{beam} = 90 GeV)

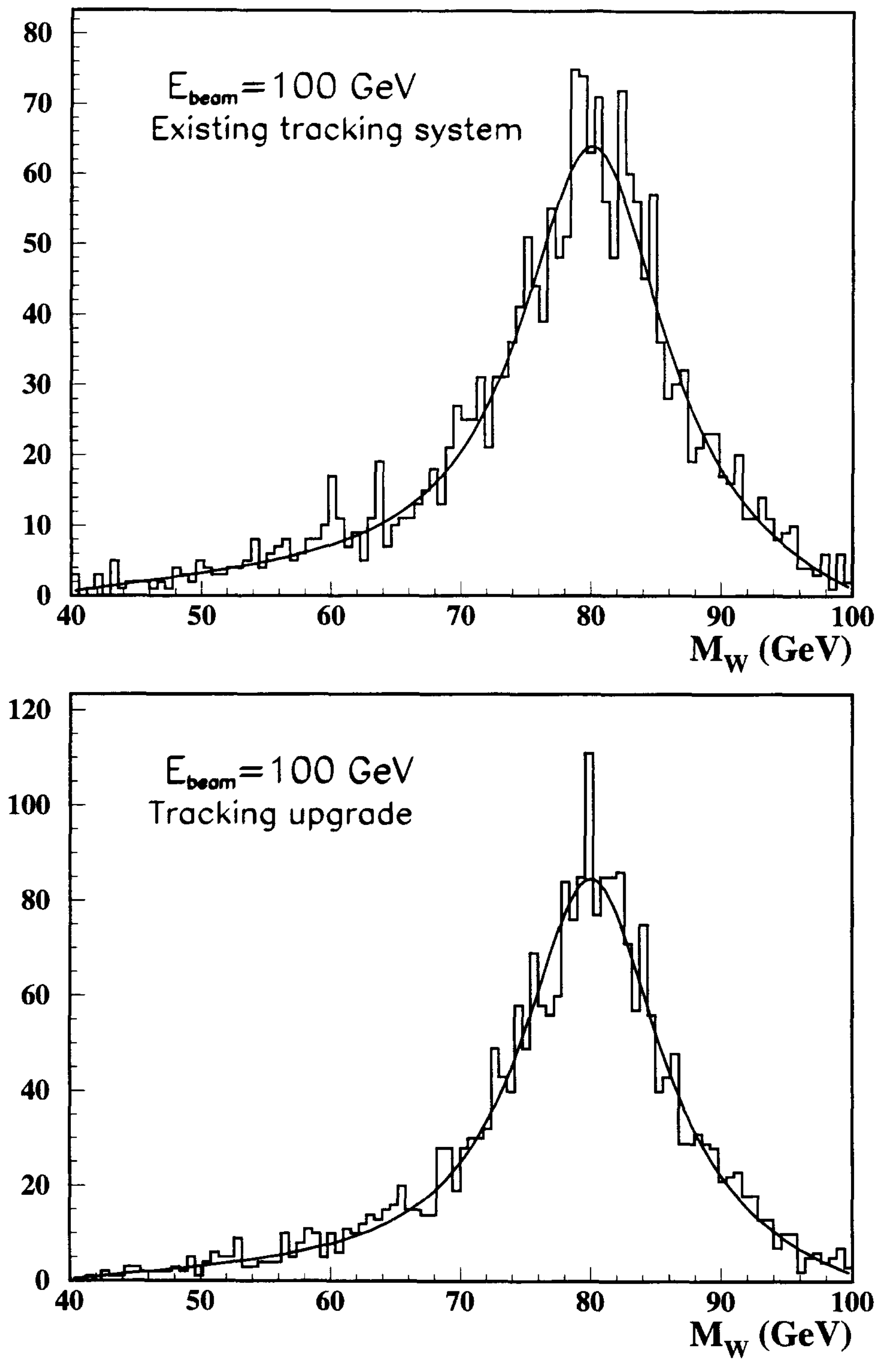

Figure 5: The reconstructed W mass in the process $e^+e^- \longrightarrow W^+W^- \longrightarrow e(\mu)\nu q\bar{q}$ (E_{beam} = 100 GeV)

cases, we obtained for the present tracker $\delta M_W = 0.136$ GeV (see Tables 4 and 5) and for the upgraded tracker $\delta M_W = 0.128$ GeV. For comparison, if we initially assume for both setups 2900 events, then after applying the cuts we have $\sim$ 2200 events for the present tracker and $\sim$ 2380 events for the upgrade (see Table 5), the resulting value of δM_W for the tracking upgrade will be 0.120 GeV. Conclusively, approximately half of the improvement of δM_W is due to the increase of statistics and the other half is due to the better performance of the upgraded tracker.

For semileptonic events the W mass reconstruction was straightforward, all the hadrons created were assigned to the same W. For pure hadronic decays ($W^+W^- \longrightarrow q\bar{q}q\bar{q}$) one has to attribute the hadrons (or jets) to a particular W. This will serve as an additional source of errors and the precision of W mass measurement using the tracker approach is expected to be lower compared to the semileptonic case, despite the larger number of events available. This is confirmed by our analysis, the expected precision for the present tracking system is $\delta M_W = 0.22$ GeV and for the upgraded tracker $\delta M_W = 0.19$ GeV.

3.3 Conclusions

The comparison of the obtained results with those presented in [5] shows that the W mass determination is most effective by using the calorimetric approach together with the kinematic fitting techniques described in [5]. When the tracker approach is used, the obtained error for W mass (δM_W) is considerably larger. The tracker approach can be used as an additional and independent method, which is complementary to the calorimetric approach.

However, by comparing the performance of the present tracker with the upgraded one gives an estimate for the expected improvement for measuring W mass. Using the tracker approach the improvement for δM_W is about 10–13%, the improvement is expected to be less for the calorimetric approach, since the result is less dependent on the performance of the trackers. Furthermore, the use of kinematic fitting techniques will further reduce the effect of the improved tracker performance.

4 Measurement of the Triple Boson Couplings

4.1 The Method

The reaction $e^+e^- \longrightarrow \mathrm{W^+W^-}$ allows direct determination of triple γWW and ZWW couplings and accordingly will provide a direct test of the underlying $SU(2)_L \times U(1)_Y$ gauge symmetry [6, 7]. The interactions among vector bosons depend on six independent coupling constants: $g_{\gamma\mathrm{WW}}$, g_{ZWW}, κ_γ, κ_Z, λ_γ, λ_Z, which determine the magnetic dipole moment

$$\mu_\mathrm{W} = \frac{e}{2M_\mathrm{W}}(1 + \kappa_\gamma + \lambda_\gamma) \tag{9}$$

and the quadrupole moment

$$Q_\mathrm{W} = -\frac{e}{M_\mathrm{W}^2}(\kappa_\gamma - \lambda_\gamma) \tag{10}$$

of the W boson.

The number of these parameters can be reduced in the framework of specific models or by symmetry requirements [6]. For simplicity we have defined

$$\delta_\mathrm{Z} = g_{\mathrm{ZWW}} - e\cot\theta_W, \tag{11}$$

$$x_\gamma = \kappa_\gamma - 1, \tag{12}$$

$$x_\mathrm{Z} = (\kappa_\mathrm{Z} - 1)g_{\mathrm{ZWW}}. \tag{13}$$

In the Standard Model:

$$g_{\mathrm{ZWW}} = g_{\gamma\mathrm{WW}} = -e\cot\theta_W, \tag{14}$$

$$\kappa_\gamma = \kappa_\mathrm{Z} = 1, \quad \lambda_\gamma = \lambda_\mathrm{Z} = 0. \tag{15}$$

We have concentrated on the following four cases [6]:

	No. of free param.	Parametrization
A	1	δ_Z – free, $x_\gamma = x_\mathrm{Z} = 0$
B	1	x_γ – free, $\delta_\mathrm{Z} = 0$, $x_\mathrm{Z} = -\frac{\sin\theta_W}{\cos\theta_W}x_\gamma$
C	1	x_γ – free, $\delta_\mathrm{Z} = \frac{x_\gamma}{\sin\theta_W\cos\theta_W}$, $x_\mathrm{Z} = -\frac{\sin\theta_W}{\cos\theta_W}x_\gamma$
D	2	δ_Z, x_γ – free, $x_\mathrm{Z} = -\frac{\sin\theta_W}{\cos\theta_W}x_\gamma$

For all cases we had $\lambda_\gamma = \lambda_\mathrm{Z} = 0$.

From the experimental results it is possible to extract the angular differential cross-section

$$\frac{d\sigma}{d(\cos\theta_\mathrm{W})}(\delta_\mathrm{Z}, x_\gamma, x_\mathrm{Z}),$$

which depends on the parameters x_γ, x_Z and δ_Z. Here θ_W stands for the polar angle of the W. Best results are obtained by using the semileptonic events ($\mathrm{W^+W^-} \longrightarrow e(\mu)\nu\mathrm{q\bar{q}}$, but also $\mathrm{W^+W^-} \longrightarrow \tau\nu\mathrm{q\bar{q}}$, if the τ does not decay hadronically). The charge of the hadronically decayed W is determined by tagging the charge of the lepton, taking into account the detector momentum resolutions. The direction of the hadronically decayed W is determined by measuring the 3–momenta of the charged decay products. The sum of the 3–momenta of the charged hadrons gives a good estimate of the W direction.

To determine the 4-momenta of final state particles, a method, which takes into account the kinematic constraints (energy and momentum conservation, W mass conservation) has been used recently [8]. The kinematical fitting method improves the resolution of measured quantities (momentum, direction etc.), but unfortunately this method is so far incapable of taking into account the initial state radiation. Therefore, in the present work we used a method based only on the reconstruction of the 3-momenta of the decay products to determine the direction of the W. The radiative corrections are then handled by introducing a correction function for the expression of differential cross section.

The obtained differential cross-section can then be fitted with a theoretical distribution. We used the theoretical distribution given in [9]. Radiative corrections were included in the theoretical formula as given in [10].

4.2 Results of Simulations

We used again $\sim$ 2900 semileptonic events with E_{beam} = 100 GeV (see section 3.2) and the following cuts were applied:

- Neutral particles and particles with $p < 0.5$ GeV were considered as undetected;
- Particles with $\theta < 24^\circ$ ($\theta > 156^\circ$) (the present tracking system) and $\theta < 13^\circ$ ($\theta > 167^\circ$) (the tracking upgrade) were considered as undetected.

The event was accepted in the analysis, if:

- An energetic lepton ($p > 20$ GeV) was observed, with $24^\circ < \theta_{lepton} < 156^\circ$ (the present tracking system) or $13^\circ < \theta_{lepton} < 167^\circ$ (the tracking upgrade).
- At least 8 charged tracks were observed.

The effect of the different cuts applied is summarized in Table 7.

	Present tracking system	Tracking upgrade
Total number of rejected events	543 (18.7%)	212 (7.3%)
Events rejected due to Cut #1	229 (7.9%)	133 (4.6%)
Events rejected due to Cut #2	305 (10.5%)	70 (2.4%)
Events rejected due to Cut #3	9 (0.3%)	9 (0.3%)

Table 7: Number of events rejected according to the different cuts (for 2900 generated events), E_{beam} = 100 GeV. Cut #1: more than 8 charged tracks; Cut #2: $\theta_{\min} < \theta_{lepton} < \theta_{\max}$; Cut #3: $p_{lept} > 20$ GeV.

The shape of the differential cross-section obtained by using the method described above, differs from the theoretical prediction, because of the following reasons.

- **Efficiency.** Events are lost, because the lepton was not detected or not enough charged tracks were detected. Proportionally more events are lost at low polar angles of the W.

- **Charge confusion.** The charge of the lepton can be determined wrongly, which leads to an error of 180° in the W direction. According to our estimates the charge confusion (over the polar angles covered by the detector) is about 2.6% for the existing tracker and about 1.0% for the tracking upgrade. The angular dependence of the charge confusion is presented in Figure 6.
- **Detector resolution.** The loss of neutral particles and the limited tracking detector angular and momentum resolutions lead to uncertainities in the reconstructed value of θ_W.

The comparison of the theoretical differential cross-section with the experimentally obtained ones is presented on Figure 7.

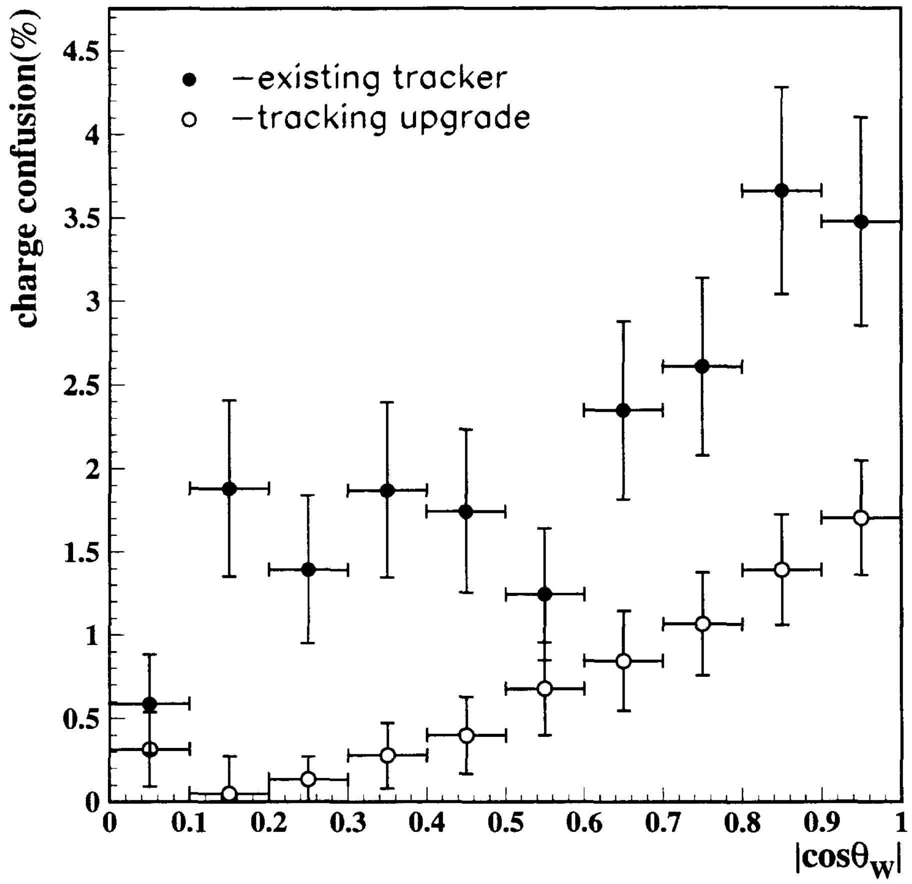

Figure 6: The charge confusion as a function of the polar angle of the W θ_W, (E_{beam} = 100 GeV).

As can be seen from Figure 7 the event losses are dependent on the polar angle of the W, therefore Monte Carlo based correction functions have to be introduced to eliminate this systematic effect.

In order to study the influence of the resolution and acceptance of the detector, we simulated 500 20-bin histograms of the angular differential cross-section with Standard Model parametrization, taking also into account:

- the Poisson-like uncertainities of the bins of the experimental histogram;

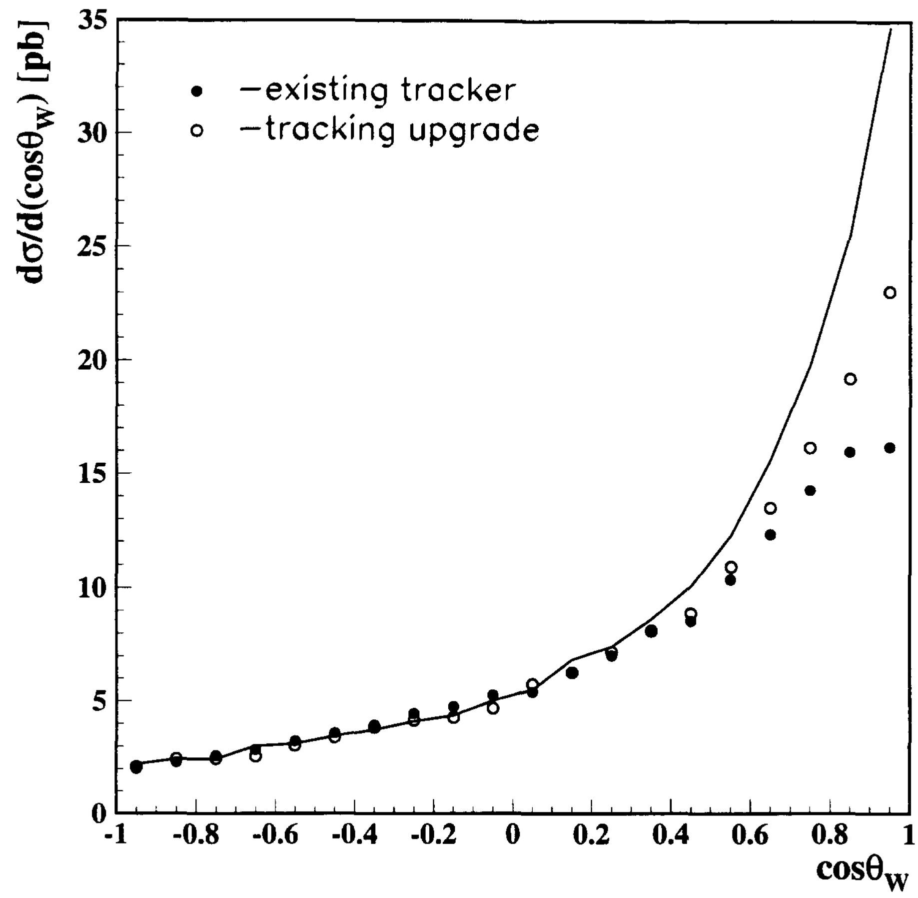

Figure 7: The angular differential cross-section $\frac{d\sigma}{d(\cos\theta_W)}$ for the process $e^+e^- \longrightarrow W^+W^-$. The solid line denotes the ideal distribution. The markers denote the uncorrected experimental distributions.

- the finite resolution ($\delta(\cos\theta_W)$) of the detector, causing severe correlations between the bins;
- the acceptance of the detector as a function of polar angle;
- the charge confusion of the W as a function of polar angle.

The obtained histograms were then fitted with a theoretical distribution.

This is equivalent to the process, where one generates 500 2900-event samples with full simulation of the trackers and thereafter carries out the same fitting procedure (correcting before for the acceptance, resolution and charge confusion effects).

For our fitting purposes we used the chisquare minimization from the MINUIT program package [11].

For the 1-parameter fits (cases A, B and C) we got 500 values for the fitted parameter, distributed around the Standard Model prediction. The distribution of the parameter values was then fitted with a Gaussian, the width of the Gaussian is a good estimate of the error of a single measurement.

The results of the 1-parameter fits are presented in Table 8.

Tracking system	$\delta(\delta_Z)$ (A)	δx_γ (B)	δx_γ (C)
The existing L3 tracking system	± 0.100	± 0.173	± 0.050
The L3 tracking upgrade	± 0.086	± 0.153	± 0.044
Improvement	14%	12%	12%

Table 8: The 95% confidence-level bounds on the fitted parameters for cases A, B and C.

Without including the charge confusion, the improvement in the precision is about 7%, therefore half of the improvement is due to better charge resolution. The other main source of improvement is the larger angular coverage of the upgraded tracker, which leads to smaller acceptance corrections and consequently to higher precision of the triple boson coupling measurements. The better momentum and angular resolutions of the upgraded tracker do not contribute significantly to the improvement in precision, since the W direction is determined indirectly by reconstructing the momenta of the caharged particles. According to our simulations $\delta(\cos\theta_W) \approx 0.10$ for both, the existing tracker and the tracking upgrade.

For the 2-parameter fit (case D) we obtained 500 pairs of x_γ and δ_Z values, presented on Figure 8.

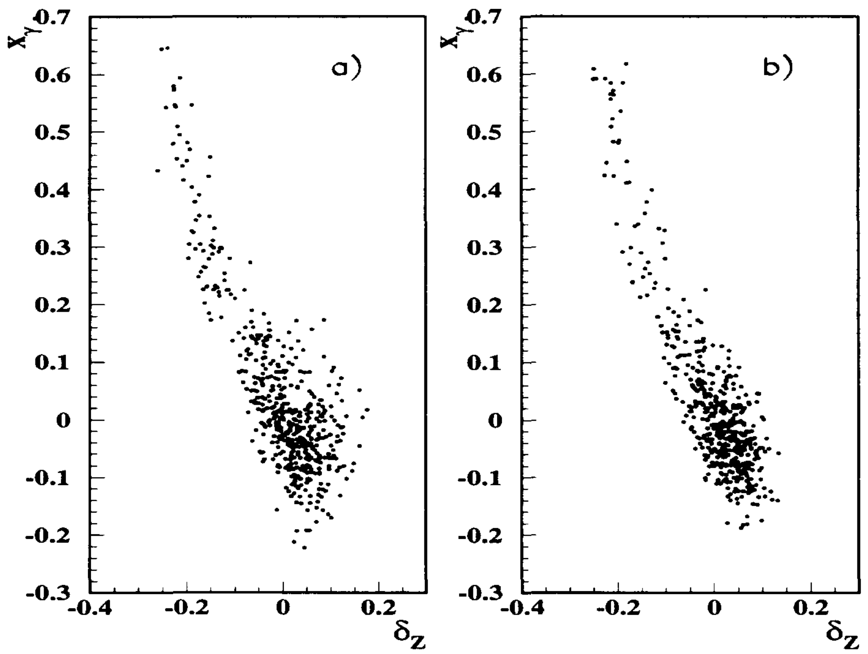

Figure 8: The results of the 500 2-parameter (x_γ, δ_Z) fits for the present tracking system (a) and the tracking upgrade (b).

The 68% and 95% confidence-level regions corresponding to the two tracker systems are presented on Figure 9. The ratio of the areas of these confidence regions is found to be 0.077 ± 0.05, which corresponds to 12% improvement in the precision of the measured triple boson coupling values.

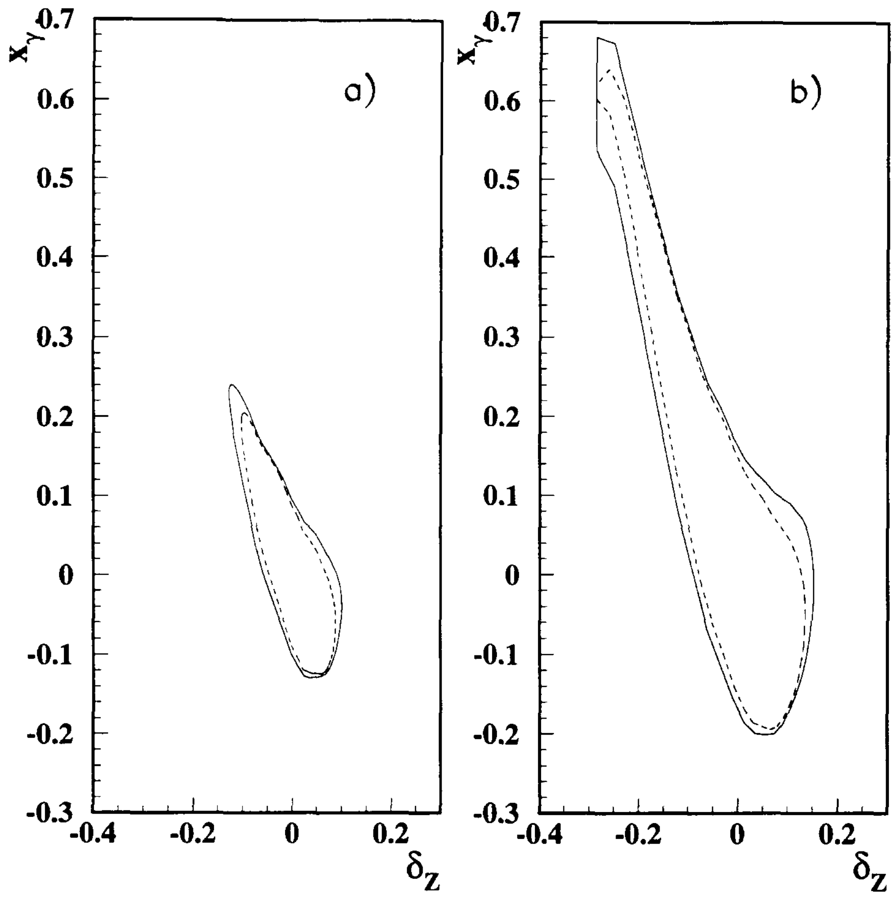

Figure 9: The 68% (a) and 95% (b) confidence-level regions for a 2-parameter fit (case D). The solid line denotes the existing tracker, the dashed line denotes the tracking upgrade.

The results obtained for the improvement of precision agree well for 1- and 2-parameter fits, but the charge confusion effects are less important for the 2-parameter case. In all studied cases the improvement is 12–14%; if one also assumes the error of a single fit to scale as $1/\sqrt{N}$, where N is the number of events in the histogram fitted, one needs to collect about 30% more data with the present tracker to achieve the precision expected from the upgraded tracker.

4.3 Conclusions

In this section we studied the effect of the tracker resolutions on the triple boson coupling measurements.

It has to be noted that the angular distribution of W's is strongly peaked in the forward direction, therefore one needs a good tracking system to effectively determine the differential cross section for W pair production. The present tracker is capable of measuring the charge of the lepton for $24^\circ < \theta_{lepton} < 156^\circ$, whereas the upgraded tracker can determine the charge of the lepton up to $13^\circ < \theta_{lepton} < 167^\circ$. Most of the improvement in precision of determining the triple boson couplings is due to the larger angular coverage of the upgraded tracker, which leads to greater statistics and smaller acceptance corrections, especially at low polar angles of the W.

The upgraded tracker will be more efficient in tagging the charge of the W, particularly at low polar angles of the lepton. The better charge tagging efficiency is another important contribution to the higher precision of the upgraded tracker in measuring the triple boson couplings.

The better momentum resolution of the upgraded tracker does not contribute significantly to the improvement in precision, the error in determining the direction of the W is approximately the same for the existing and upgraded tracker (if we forget the charge confusion for a moment).

Conclusively it can be said that if the existing tracker is not replaced by the upgraded one, 30% more data have to be gathered to obtain the same precision as expected from the upgraded tracker for the triple boson coupling measurements.

References

[1] K. Hagiwara *et al.*, Nucl. Phys. B282, 253.

[2] W. Beenakker, A. Denner Standard–Model Predictions for W-Pair Production in Electron–Positron Collisions, DESY 94–051.

[3] M. Juntunen, *et al.* The Silicon Tracking Upgrade of L3 for LEP200, HU–SEFT RD 1994–02.

[4] A. Böhm and W. Hoogland, Proceedings of the ECFA Workshop on LEP-200, Aachen, Germany, 29 September-1 October 1986, CERN 87-08, 1988.

[5] W Mass Working Group, L3 Note 1474 (1994).

[6] M. Bilenky, *et al.* Nucl. Phys. B409 (1993), pp.22–68.

[7] Bielefeld–Montpellier–Thessaloniki Collaboration Proceedings of the Workshop "e^+e^- Collisions at 500 GeV: the Physics Potential", DESY 92–123, pp.735–755.

[8] B. N. Jin, M. Pohl, L3 Note 1479 (1993).

[9] C. L. Bilchak, J. Stroughair, Phys. Rev. D, Vol.30, pp.1881–1889.

[10] R. Philippe, Phys. Rev. D, Vol.26, pp.1588–1599.

[11] CERN Program Library Writeup D506.